PROCEEDINGS OF SCIENCE

Yonetoku relation of Fermi-GBM and Swift-BAT gamma-ray bursts

Feraol Fana Dirirsa*
Centre for Astro-Particle Physics (CAPP) and Department of Physics, University of Johannesburg P.O. Box 524, Auckland Park 2006, South Africa
E-mail: fdirirsa@uj.ac.za

Soebur Razzaque
Centre for Astro-Particle Physics (CAPP) and Department of Physics, University of Johannesburg P.O. Box 524, Auckland Park 2006, South Africa
E-mail: srazzaque@uj.ac.za

We study empirical relation between the intrinsic peak energy $E_{\rm i,p}$ of the νF_ν spectrum and the isotropic peak luminosity ($L_{\rm iso}$) of Gamma-ray burst (GRB) prompt emission in the cosmological source frame. The $E_{\rm i,p}$ and $L_{\rm iso}$ are computed for all long GRBs detected by the *Fermi* Gamma-ray Burst Monitor (GBM) and *Swift*-Burst Alert Telescope (BAT) until the end of December 2017, for which redshift is measured and which has a well defined time-integrated peak spectrum. The GBM has larger sky coverage than BAT but is less sensitive, therefore GRBs that trigger GBM are visible to the BAT. It is very interesting to study the $E_{\rm i,p}$–$L_{\rm iso}$ correlation using the samples obtained from both these detectors because each has its own advantages. In both samples, we found that the $E_{\rm i,p}$ is strongly correlated with the $L_{\rm iso}$. Using the slope and normalization obtained from our fits, we constructed the Hubble diagram and estimate the cosmological parameters for the GRB samples, and also by combining our GRB samples together with the latest Union Supernovae (SNe) type Ia data.

6th Annual Conference on High Energy Astrophysics in Southern Africa
August, 1–3 2018
Parys, Free State, South Africa

*Speaker.

PoS(HEASA2018)012

1. Introduction

Since the launch of the *Fermi* Gamma-ray Space Telescope on 2008 June 10 and the *Swift* satellite on 2004 November 20, a significant number of GRBs have been observed by both the *Fermi* Gamma-ray Burst Monitor (GBM, 8 keV–40 MeV) [1] and the *Swift*-Burst Alert Telescope (BAT, 15–350 keV) [2]. Observations by these telescopes have allowed to study the spectral properties and energy of GRBs detected up to very high redshifts [3]. We study an empirical relation between the intrinsic peak energy $E_{\rm i,p}$ of the νF_ν spectrum and the isotropic peak luminosity $L_{\rm iso}$ in the cosmological source frame, the so-called Yonetoku relation [4]. Our sample comprises all long GRBs (lGRBs) with measured redshift reported in the *Fermi*-GBM [5, 6, 7] and *Swift*-BAT [8] catalogs, until December 2017. For these GRBs, we derive, where possible, the $E_{\rm i,p}$ and the $L_{\rm iso}$ from the best-fit parameters of spectral fit. In order to compute these observables, we consider a one-second ($T_{\rm peak}$) time integrated spectral analysis. It is a time when the light curve of GRB prompt emission peaks, and which is measured from the trigger time. Since, the GBM has larger sky coverage and is less sensitive than the BAT, some of the GRBs that trigger GBM are also visible to the BAT. The spectral peak energy and the flux of BAT GRBs, because it is sensitive to a narrower and lower energy range, are lower compared to the GBM GRBs. The BAT may miss the high energy photons to be used for the spectral analysis as a result. This may lead to finding different spectral peak energy for the same burst detected by GBM and BAT instruments.

The correlations between the spectral peak energy and energy output for lGRBs have important implications both for theoretical understanding of the burst physics and for application of GRBs possibly as cosmological tools [9, 10, 11]. If GRBs can be standardized, similarly to type Ia SNe [12, 13], they could potentially be used as cosmological tools to probe the distant Universe. Following the finding of the Yonetoku relation, much efforts have been made by several independent authors [14, 15] to investigate whether this relation has a physical origin or it is due to an instrumental selection effect (or bias) [16]. To date, there is no clear consensus reached on the physical interpretation of these correlations [17, 18]. Recently, however, interesting progress has been made to answer this question by studying the comoving properties of GRBs [19, 20]. The discovery of small dispersion/outliers with a tighter correlation around the power law best-fit line of the Yonetoku relation is promising. Despite this discussion, the $E_{\rm i,p}$–$L_{\rm iso}$ correlation has been proposed as a possible mechanism to constrain cosmological parameters [9, 21].

In this work, we study the validity and stability of the Yonetoku relation [4], using samples of lGRBs from the BAT and GBM instruments. The calibrated parameters obtained from this correlation have been used to construct the Hubble's diagram and estimate the cosmological parameters for the lGRB samples alone and together with the latest Union Supernovae SNe type Ia data [22].

2. Sample selection

As of December 2017, the *Swift*-BAT has detected 1192 GRBs [8], of which about 35% have measured redshifts. In the case of the *Fermi*-GBM detected 2232 GRBs [5, 6, 7], only $\sim 5\%$ have measured redshift. Since the energy band of the BAT is narrow (i.e., 15–150 keV), the spectral peak energy ($E_{\rm p}$) of GRBs are sometimes outside of the energy band. So, we cannot precisely characterize it. Some soft GRBs (i.e., low power-law spectral index) have $E_{\rm p}$ below the energy threshold of the BAT energy range. In addition, a simple power law (PL) is an acceptable spectral fit for most GRBs detected by BAT, which do not provide E_p. This reduces the number of GRBs with measured redshift in our analysis of $E_\mathrm{i,p}$–L_iso correlation. So, we have identified 38 GRBs (hereafter, S_BAT) which were modeled by a power law with an exponential cutoff (PLEC). We have also identified 76 GBM GRBs (hereafter, F_GBM) for which their spectral fitting parameters are constrained from the spectral models such as the Band function [23], smoothly broken power law [24] and PLEC. In the joint $F_\mathrm{GBM}+S_\mathrm{BAT}$ sample, we have excluded 12 GRBs from the BAT sample which are simultaneously detected by both GBM and BAT instruments.

3. Intrinsic peak energy and isotropic peak luminosity

In this section we discuss the computation of $E_\mathrm{i,p}$ and L_iso for different GRB samples detected by the BAT and GBM instruments. After measuring a spectroscopic or photometric redshift of a GRB, one can correct for cosmological effects and infer its rest frame spectral peak energy as $E_\mathrm{i,p} = E_\mathrm{p}(1+z)$. The 1-second isotropic peak luminosity L_iso is calculated in the cosmological source frame as

$$L_\mathrm{iso} = 4\pi d_\mathrm{L}^2 F_\mathrm{bolo},\ \mathrm{erg/s}, \tag{3.1}$$

where $F_\mathrm{bolo} = \int_{E_{1/1+z}}^{E_2/1+z} EN(E)dE$ [erg cm^{-2} s^{-1}] is the measured peak bolometric flux integrated over the energy range from $E_1 = 1$ keV to $E_2 = 10^4$ keV. Here $N(E)$ is the 1-second time-integrated spectrum of the acceptable fitting models (i.e., Band, PLEC and SBPL). Assuming a flat ΛCDM model (i.e., $\Omega_\Lambda + \Omega_\mathrm{m} = 1$), the luminosity distance (d_L) can be expressed with Hubble constant H_0 (km s^{-1} Mpc^{-1}) as $d_\mathrm{L} = (1+z)cH_0^{-1}\int_0^z dz'/\left((1-\Omega_\Lambda)(1+z')^3+\Omega_\Lambda\right)^{1/2}$, where Ω_Λ and Ω_m are the dark energy and dark matter densities at present time, respectively. The uncertainty σ_{L_iso} of Eq. (3.1) can be computed with a propagation of error approach using errors on parameters obtained from the best-fit spectral analysis. The uncertainty for each parameter has been estimated at 90% confidence level as reported in the GBM [5, 6, 7] and BAT GRB [8] catalogs.

4. The Yonetoku relation

The phenomenological L_iso–$E_\mathrm{i,p}$ correlation can be described by a simple power law as

$$L_\mathrm{iso} = k\left(\frac{E_\mathrm{i,p}}{E_\mathrm{0,dec}}\right)^m L_\mathrm{0,iso}, \tag{4.1}$$

where $E_\mathrm{0,dec}$ is the de-correlation energy at which the error on $E_\mathrm{i,p}$ becomes small, m is the index of PL, k is a proportionality constant and $L_\mathrm{0,iso} = 10^{52}$ erg s^{-1}. For each GRB in the samples, we have computed $E_\mathrm{i,p}$ and L_iso using Eq. (3.1) in the 1 keV–10 MeV energy range. In such a way that Eq. (3.1) takes the linearized form

$$y = mx + k \tag{4.2}$$

where $y \equiv \log(L_\mathrm{iso}/L_\mathrm{0,iso})$ and $x \equiv \log(E_\mathrm{i,p}/E_\mathrm{0,dec})$. The error on y (Eq. (4.2) is estimated as $\sigma_\mathrm{y}^2 = \sigma_\mathrm{k}^2 + m^2\sigma_\mathrm{x}^2 + \sigma_\mathrm{m}^2 x^2 + \sigma_\mathrm{ext}^2$. Here the systematic uncertainties $\sigma_{\mathrm{x_i}}$ and $\sigma_{\mathrm{y_i}}$ are the errors on the x and y data, respectively. σ_ext is an extrinsic systematic error, which is treated as an unknown physical parameter. This may account for hidden parameters related to the physical origin of the Yonetoku relation. In order to constrain $\sigma_{\rm ext}$ and coefficients of the $L_{\rm iso}$-$E_{\rm i,p}$ correlation, we apply the maximum likelihood statistical method [25] given by

$$L(m,k,\sigma_{\rm ext}) = \frac{1}{2}\sum_i^N \ln(\sigma_{\rm ext}^2 + \sigma_{y_{\rm i}}^2 + m^2\sigma_{x_{\rm i}}^2) + \frac{1}{2}\sum_i^N \frac{(y_{\rm i} - mx_{\rm i} - k)^2}{(\sigma_{\rm ext}^2 + \sigma_{y_{\rm i}}^2 + m^2\sigma_{x_{\rm i}}^2)}. \tag{4.3}$$

We mazimize this function to find the best-fit values of the parameters m, k and $\sigma_{\rm ext}$. The obtained results are listed in Tab. 1 for the $F_{\rm GBM}$ and $S_{\rm BAT}$ samples, and for the combination of the two samples. To determine uncertainties of a fit parameter $q_{\rm i}$, we apply the log likelihood function $-\ln\mathscr{L}(m,k,\sigma_{\rm ext}) \equiv L(m,k,\sigma_{\rm ext})$ to fit the x and y data with Eq. (4.2) as in [26]. A marginalized likelihood function $\mathscr{L}_{\rm i}(q_{\rm i})$ has been evaluated by integrating over other parameters. Then the median value for the parameter $q_{\rm i,med}$ was found from the integral $\int_{q_{\rm i,min}}^{q_{\rm i,med}} \mathscr{L}_{\rm i}(q_{\rm i})dq_{\rm i} = \frac{1}{2}\int_{q_{\rm i,min}}^{q_{\rm i,max}} \mathscr{L}_{\rm i}(q_{\rm i})dq_{\rm i}$, where $q_{\rm i,min}$ and $q_{\rm i,max}$ are the minimum and maximum values of the parameters, respectively. The 1σ or 68.27% confidence interval $(q_{\rm i,l}, q_{\rm i,h})$ of the parameters are then found

Table 1: The best-fit parameters of the $E_{\rm i,p}$–$L_{\rm iso}$ correlation of $F_{\rm GBM}$, $S_{\rm BAT}$ and the joint $F_{\rm GBM}+S_{\rm BAT}$ samples. The $\rho_{\rm E_{i,p},L_{iso},z}$ and $\rho_{\rm E_{i,p},L_{iso}}$ are the partial and the Pearson correlation coefficients, respectively.

lGRB samples	No. of GRBs	$\rho_{\rm E_{i,p},L_{iso}}$	$\rho_{\rm E_{i,p},L_{iso},z}$	m	k	$\sigma_{\rm ext}$
$F_{\rm GBM}$	76	0.67	0.52	1.56 ± 0.35	52.61 ± 0.12	0.53 ± 0.09
$S_{\rm BAT}$	38	0.83	0.75	2.69 ± 0.65	52.50 ± 0.18	0.31 ± 0.15
$F_{\rm GBM}+S_{\rm BAT}$	102	0.70	0.63	1.60 ± 0.29	52.48 ± 0.10	0.54 ± 0.08

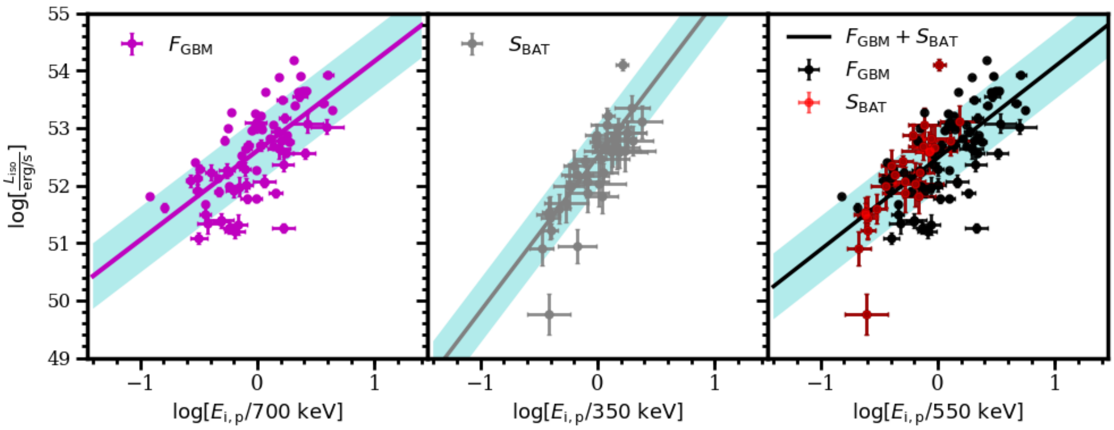

Figure 1: *Left panel* – The $E_{\rm i,p}-L_{\rm iso}$ correlation for $F_{\rm GBM}$ sample (magenta). *Middle panel* – The $E_{\rm i,p}-L_{\rm iso}$ correlation for $S_{\rm BAT}$ sample (grey). *Right panel* – The $E_{\rm i,p}-L_{\rm iso}$ correlation for the combined $F_{\rm GBM}+S_{\rm BAT}$ sample, which are not simultaneously detected by GBM and BAT.

by solving the integral [25] given by

$$\int_{q_{\rm i,l}}^{q_{\rm i,med}} \mathscr{L}_{\rm i}(q_{\rm i})dq_{\rm i} = \frac{1-\eta}{2}\int_{q_{\rm i,min}}^{q_{\rm i,max}} \mathscr{L}_{\rm i}(q_{\rm i})dq_{\rm i}\,; \int_{q_{\rm i,med}}^{q_{\rm i,h}} \mathscr{L}_{\rm i}(q_{\rm i})dq_{\rm i} = \frac{1-\eta}{2}\int_{q_{\rm i,min}}^{q_{\rm i,max}} \mathscr{L}_{\rm i}(q_{\rm i})dq_{\rm i} \tag{4.4}$$

where η = 0.6827. Hence, we calculate the mean of the upper and lower uncertainties for each parameter. We have plotted the Yonetoku relation in Fig. 1 by using the best-fit parameters listed in Tab. 1 for $F_{\rm GBM}$ and $S_{\rm BAT}$ samples and the joint GBM and BAT sample. We see that the best-fit index ($m = 2.69 \pm 0.65$) for the $S_{\rm BAT}$ sample is steeper than the slopes of the $F_{\rm GBM}$ ($m = 1.56 \pm 0.35$) and the joint $S_{\rm BAT} + F_{\rm GBM}$ (m = 1.60 $\pm$ 0.29) samples reported in Tab. 1. At the low luminosities and for $S_{\rm BAT}$ and $S_{\rm BAT} + F_{\rm GBM}$ samples, we find a mild shift of the population away from the Yonetoku relation in the direction of higher $E_{\rm i,p}$ (see the right panel of Fig. 1). This resulted in a correlation line with steeper (harder) slope at the specified luminosity range. A possible explanation of these inconsistencies is that the Yonetoko relation may largely be due to an observational bias. Note that it is more difficult to detect weak hard bursts as those have fewer photons. This is manifested by the fact that the index is larger for Swift that has a softer detection band. For a sample of $S_{\rm BAT}$ the partial correlation coefficient $\rho_{\rm E_{i,p},L_{iso},z} = 0.75$ and the Pearson correlation coefficient $\rho_{\rm E_{i,p},L_{iso}}$ = 0.83. The degree of this correlation is higher than the other $F_{\rm GBM}$ and the combined $S_{\rm bat}$ + $F_{\rm GBM}$ samples.

5. Constraints on cosmological parameters and the extended Hubble diagram

Once the parameters are obtained by fitting the linearized Yonetoku relation, we can use lGRBs to constrain the cosmological parameters. Our procedure is the following. We invert the relation in Eq. (4.1) to obtain $d_{\rm L}$, which can be expressed in terms of $L_{\rm iso}$ and $F_{\rm bolo}$ as $d_{\rm L} = \left[(1+z)L_{\rm 0,iso}10^k/(4\pi F_{\rm bolo})\left(E_{\rm i,p}/E_{\rm 0,dec}\right)^m\right]^{1/2}$. Using the computed $d_{\rm L}$ for each GRB, we construct the Hubble's diagram from the distance modulus $\mu(z) = 5\log(d_{\rm L}/1\,{\rm Mpc}) + 25$. Then the distance modulus related to the power law form of Yonetoku relation in Eq. (4.1) can be written as

$$\mu = \frac{5}{2}\log\left[\frac{L_{\rm 0,iso}}{4\pi F_{\rm bolo}}\left(\frac{E_{\rm i,p}}{E_{\rm 0,dec}}\right)^m\right] + \frac{5}{2}k - 5\log\left(1{\rm Mpc}\right) + 25. \tag{5.1}$$

Here the μ uses all the fitting parameters obtained from the $E_{\rm i,p} - L_{\rm iso}$ correlation. The variance of μ is computed by using error propagation method and is given by

$$\sigma_\mu^2 = \left(\frac{\partial\mu}{\partial\log L_{\rm iso}}\right)^2\sigma^2_{\log L_{\rm iso}} + \left(\frac{\partial\mu}{\partial F_{\rm bolo}}\right)^2\sigma^2_{F_{\rm bolo}} = \left(\frac{5}{2}\sigma_{\log L_{\rm iso}}\right)^2 + \left(\frac{5}{2\,\ln 10}\frac{\sigma_{F_{\rm bolo}}}{F_{\rm bolo}}\right)^2, \tag{5.2}$$

where $\sigma_{\log L_{\rm iso}}$ is the propagated uncertainty on $L_{\rm iso}$ computed from $\sigma_{\rm y}$ of Eq. (4.2) and yield $\sigma^2_{\log L_{\rm iso}} = \left(\sigma_{\rm m}\log(E_{\rm i,p}/E_{\rm 0,dec})\right)^2 + \left(m\sigma_{\rm E_{i,p}}/(\ln 10 E_{\rm i,p})\right)^2 + \sigma_{\rm k}^2 + \sigma_{\rm ext}^2$. One can plot the Hubble diagram using μ (Eq. 5.1) and its uncertainty σ_μ (Eq. 5.2). The parameters of a flat ΛCDM cosmological model can be constrained by using the GRB sample or GRB sample together with SNe U2.1 sample [22]. The best-fit cosmological parameters can be obtained by minimization of the χ^2 expression given by

$$\chi^2(H_0,\Omega_\Lambda) = \sum_{i=0}^{N}\frac{\left(\mu(z) - \mu^{\rm th}(z;H_0,\Omega_\Lambda)\right)^2}{\sigma^2_{\mu_{(z)}}}, \tag{5.3}$$

where $\mu(z)$ is the distance modulus obtained from Eq. (5.1), $\sigma_{\mu_{(z)}}$ is the uncertainty of distance modulus obtained from Eq. (5.2) and $\mu^{\rm th}(z,H_0,\Omega_\Lambda) = 5\log(d_{\rm L}(H_0,\Omega_\Lambda)/1\,{\rm Mpc}) + 25$ is a theoretically predicted value of the distance modulus.

PoS(HEASA2018)012

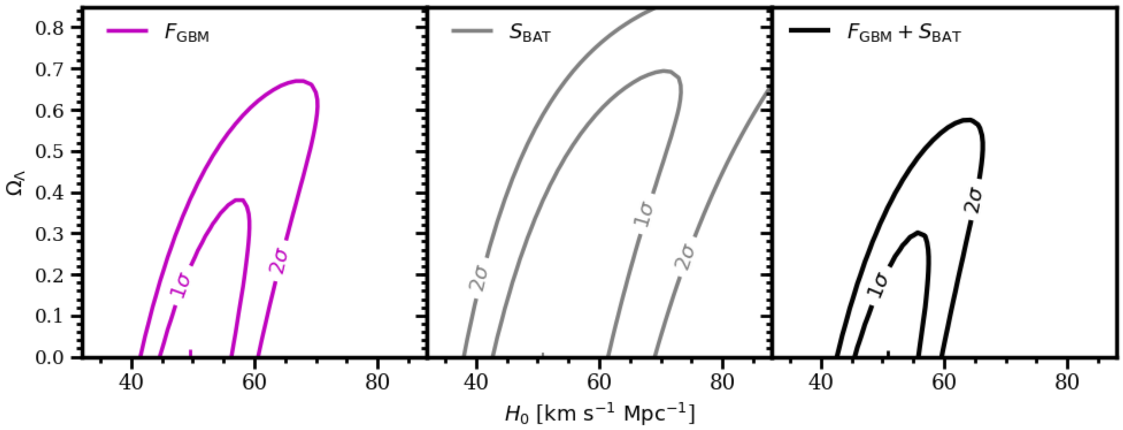

Figure 2: Constraints on the cosmological parameters from fitting of the Yonetoku relation for different samples of lGRBs. *Left panel* – The Ω_Λ and H_0 obtained from $F_{\rm GBM}$ sample (magenta). *Middle panel* – The Ω_Λ and H_0 obtained from the $S_{\rm BAT}$ sample (grey). *Right panel* – The $\Omega_\Lambda - H_0$ obtained from the $F_{\rm GBM}$+$S_{\rm BAT}$ sample (black). The 1σ and 2σ confidence levels of the pair of cosmological parameters determined by following $\Delta\chi^2 \equiv \chi^2 - \chi^2_{\rm min} \leq 2.30$ and 6.18, respectively.

We have performed a χ^2 analysis to constrain cosmological parameters using lGRBs and applied it to different samples depending on the coefficients of the $E_{\rm i,p}$–$L_{\rm iso}$ relation. Then we considered all possible values of the cosmological parameters to plot the likelihood contours in the (Ω_Λ, H_0) plane at the 1σ and 2σ confidence levels as shown in Fig. 2. The values of these parameters at 1σ confidence level for different samples are reported in Tab. 2. The large contours on the cosmological parameters are direct results of the errors on the correlation coefficients in Yonetoku relation. The combination of GRBs and SNe type Ia data can potentially be used as a probe of the Hubble diagram. In our analysis, we used the recent 580 SNe U2.1 sample [22] that covers the redshift from 0.015 to 1.414. Note that Riess et al. [27] obtained a different value of H_0 than shown in Tab. 2, using other different samples. In the left panel of Fig. 3, we plotted the likelihood contours of SNe U2.1 with a measured value of $H_0 \simeq 69.99$ km s^{-1} Mpc^{-1} and $\Omega_\Lambda \simeq 0.72$, and the likelihood contour of $F_{\rm GBM}+S_{\rm BAT}$+SNe U2.1 sample with a measured value of $H_0 \simeq 69.91$ km s^{-1} Mpc^{-1} and $\Omega_\Lambda \simeq 0.72$ in 1σ confidence intervals. The best-fit value in 1σ confidence level is consistent with the Planck values [28]. However, the errors on parameters are rather large that may have arised due to the large extrinsic systematics scattering associated with the hidden parameters related to the physical origin of the Yonetoku relation. The right panel of Fig. 3 shows the Hubble diagram constructed with the SNe U2.1 together with $F_{\rm GBM}$ and $S_{\rm BAT}$ samples. The black line is plotted using the estimated cosmological parameters $H_0 = 69.908$ km s^{-1} Mpc^{-1} and $\Omega_\Lambda = 0.715$

Table 2: Constraints on H_0 [km s^{-1} Mpc^{-1}] and Ω_Λ in 1σ confidence level in the flat Universe.

Samples	$F_{\rm GBM}$	$S_{\rm BAT}$	$F_{\rm GBM}+S_{\rm BAT}$	SNe U2.1	$F_{\rm GBM}+S_{\rm BAT}$+SNe U2.1
H_0	$49.59^{+9.71}_{-5.00}$	$50.82^{+22.83}_{-8.17}$	$50.82^{+6.89}_{-5.49}$	$69.99^{+0.54}_{-0.53}$	$69.91^{+0.53}_{-0.52}$
Ω_Λ	-	-	-	0.723 ± 0.03	0.715 ± 0.03

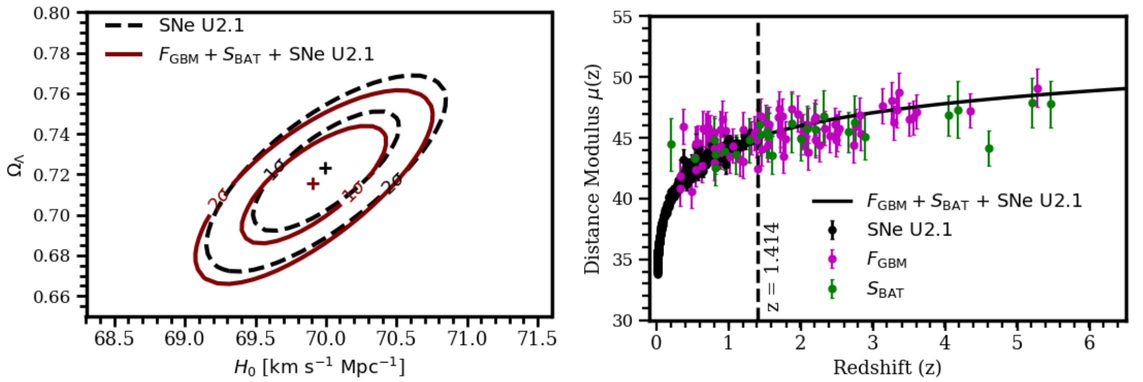

Figure 3: *Left panel* – Contours of likelihood in the (H_0, Ω_Λ) plane for SNe U2.1 (black color) and SNe U2.1 with the combined $F_{GBM} + S_{BAT}$ (maroon color) samples in 1σ and 2σ confidence levels. The plus signs show the location of the best-fit. *Right panel* – Combined SNe and GRB Hubble diagram for the $F_{GBM} + S_{BAT}$ + SNe U2.1 sample. The black solid line represents the distance moduli $\mu(z)$ obtained with the best-fit cosmological parameters obtained from $F_{GBM} + S_{BAT}$ + SNe U2.1 data. The vertical broken line is plotted at the maximum redshift $z = 1.414$ of the SNe U2.1 data.

obtained from these joint analyses.

6. Summary

The *Swift*-BAT and *Fermi*-GBM GRBs with known redshift have been used to analyze the L_{iso}–$E_{i,p}$ correlation. The L_{iso} and $E_{i,p}$ are computed by using the parameters obtained from the best-fit models of spectral analysis reported in the GBM and BAT GRB catalogs. The best-fit of the Yonetoku relation for the joint $F_{GBM} + S_{BAT}$ sample can be expressed as

$$\frac{L_{iso}}{\text{erg s}^{-1}} = 10^{52.48\pm0.10} \left(\frac{E_{i,p}}{550\ \text{keV}}\right)^{1.60\pm0.29} .$$

This result is consistent with previous work of [21]. The phenomenological correlation of $E_{i,p}$ and L_{iso} also showed a strong correlation. For instance, the Pearson correlation coefficient for the BAT sample is 0.83, which is higher than the GBM sample. Using the coefficients of the correlation obtained from the analyzed samples of GRBs and also by combining with the recent SNe type Ia data, we construct an extended GRB Hubble diagram up to a redshift of z = 5.4636. Our fit to the combined GRB sample ($F_{GBM} + S_{BAT}$) with the SNe U2.1 sample resulted in good fit to the cosmological parameters of $H_0 = 69.91^{+0.53}_{-0.52}$ km s^{-1} Mpc^{-1} and $\Omega_\Lambda = 0.715 \pm 0.03$. This analysis is dominated by the SNe U2.1 sample due to smaller error bars. However, with the present GBM and BAT samples of lGRBs alone, Ω_Λ and H_0 cannot be meaningfully constrained since the errors on parameters are rather large that arise due to the large extrinsic systematics scattering associated to the sample.

References

[1] Meegan C *et al.* 2009 *The Astrophysical Journal* **702** 791

[2] Gehrels N *et al.* 2004 *The Astrophysical Journal* **611** 1005

[3] Gehrels N and Razzaque S 2013 *Frontiers of Physics* **8** 661–678

[4] Yonetoku D *et al.* 2004 *The Astrophysical Journal* **609** 935–951

[5] Gruber D *et al.* 2014 *The Astrophysical Journal Supplement Series* **211** 12

[6] Von Kienlin A *et al.* 2014 *The Astrophysical Journal Supplement Series* **211** 13

[7] Bhat P N *et al.* 2016 *The Astrophysical Journal Supplement Series* **223** 28

[8] Lien A *et al.* 2016 *The Astrophysical Journal* **829** 7

[9] Ghirlanda G, Ghisellini G and Firmani C 2006 *New Journal of Physics* **8** 123

[10] Cardone V, Capozziello S and Dainotti M 2009 *Monthly Notices of the Royal Astronomical Society* **400** 775–790

[11] Tsutsui R, Nakamura T, Yonetoku D, Murakami T, Kodama Y and Takahashi K 2009 *Journal of Cosmology and Astroparticle Physics* **8** 015

[12] Riess A G *et al.* 1998 *Astronomical Journal* **116** 1009–1038

[13] Perlmutter S *et al.* 1999 *The Astrophysical Journal* **517** 565–586

[14] Ghirlanda G *et al.* 2012 *Monthly Notices of the Royal Astronomical Society* **422** 2553–2559

[15] Nava L, Ghirlanda G and Ghisellini G 2009 *AIP Conference Proceedings* vol 1133 (AIP) pp 350–355

[16] Dainotti M G and Amati L 2018 *Publications of the ASP* **130** 051001

[17] Eichler D and Levinson A 2004 *The Astrophysical Journal Letter* **614** L13–L16

[18] Levinson A and Eichler D 2005 *The Astrophysical Journal Letters* **629** L13–L16

[19] Panaitescu A 2009 *Monthly Notices of the Royal Astronomical Society* **393** 1010–1015

[20] Ghirlanda G *et al.* 2012 *Monthly Notices of the Royal Astronomical Society* **420** 483–494

[21] Schaefer B E and Collazzi A C 2007 *The Astrophysical Journal Letters* **656** L53–L56

[22] Suzuki N, *et al.* 2012 *The Astrophysical Journal* **746** 85

[23] Band D *et al.* 1993 *The Astrophysical Journal* **413** 281–292

[24] Ryde F 1998 *arXiv preprint astro-ph/9811462*

[25] D'Agostini G 2005 *arXiv preprint physics/0511182*

[26] Demianski M and Piedipalumbo E 2011 *Monthly Notices of the Royal Astronomical Society* **415** 3580–3590

[27] Riess A G, *et al.* 2018 *The Astrophysical Journal* **861** 126

[28] Ade P A *et al.* 2016 *Astronomy & Astrophysics* **594** A13